

CONTACT PROBLEM FOR A PNEUMATIC TIRE INTERACTING WITH A RIGID FOUNDATION

E. I. Grigolyuk,* G. M. Kulikov,**
and S. V. Plotnikova**

Keywords: multilayered shell, finite-element method, contact problem, tire

Based on mixed finite-element approximations, a numerical algorithm is developed for solving a geometrically nonlinear contact problem for a prestressed multilayered Timoshenko-type shell undergoing arbitrarily large displacements and rotations. As unknowns, six displacements of faces of the shell are taken, which allows one to use principally new relationships for components of the Green–Lagrange strain tensor in curvilinear orthogonal coordinates, exactly representing arbitrarily large displacements of the shell as a rigid body. As an example, a tire interacting with a rigid foundation is considered.

Introduction

The problem of developing numerical algorithms and a software for solving contact problems for multilayer composite shells of revolution with reference to tires, whose physico-mechanical properties are highly inhomogeneous on the macroscopic level, has not yet been finally solved to date. The spatial character of stress and strain fields in the case of a rather general kind of anisotropy necessitates us to considerably complicate the problem in order to obtain acceptable results [1]. The extensive way of calculating tires, which is based on the three-dimensional theory of elasticity and the finite-element method with a fine mesh and has been widely used during the last years, is important in checking calculations of already designed tires in order to finally refine their structural scheme [2, 3]. However, the initial stage in tire design should be carried out by using high-speed programs based on PC-oriented shell models of various complexity.

Unfortunately, during the last years, the current achievements in the theory of composite shells were used for solving the problems of contact interaction of tires only in few studies [4-6], where the transverse compression of tires was not taken into account. Moreover, the present authors are unaware of results on numerical investigations of the effect of anisotropy on the contact zone between the tire and a foundation and on the distribution of contact pressure. Some experimental and preliminary calculation data [7] indicate that the contact zone is asymmetric. The present study is dedicated to the solution of these questions.

Let us consider a thin shell composed of N elastic anisotropic layers with initial stresses. By initial stresses we understand the stresses arising in the shell in the initial state, i.e., before the onset of the deformation we are interested in. We assume that, at each point of the shell, there is a surface of elastic symmetry parallel to the reference surface. As a reference surface, S ,

*Moscow State Technical University “MAMI,” Russia. **Tambov State Technical University, Russia. Translated from *Mekhanika Kompozitnykh Materialov*, Vol. 40, No. 5, pp. 661-674, September-October, 2004. Original article submitted March 8, 2004.

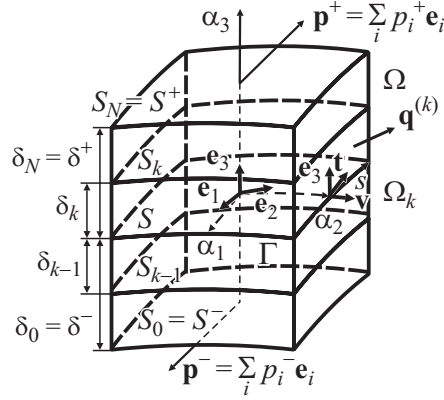


Fig. 1. Scheme of a multilayered shell.

we take either the inner surface of some k th layer or the interface between the layers, which is referred to curved orthogonal coordinates α_1 and α_2 measured along the lines of main curvatures. The transverse coordinate α_3 is measured in the direction of increasing external normal to the reference surface S (Fig. 1).

In what follows, \mathbf{e}_1 and \mathbf{e}_2 are the unit tangent vectors of coordinate lines α_1 and α_2 , \mathbf{e}_3 is the unit normal vector, A_α are the Lamé parameters, k_α are the curvatures of coordinate lines, h is the total thickness of the shell, h_k is the thickness of a k th layer, δ_k is the distance from the surface S to the upper boundary surface of the k th layer S_k , u_i are the displacements of points of the shell, $\varepsilon_{ij}^{\text{GL}}$ are the components of the Green–Lagrange strain tensor, $\varepsilon_{ij}^{\text{AS}}$ are the components of the displacement-independent strain tensor, $\tau_{ij}^{(k)}$ are the components of the Cauchy tensor of initial stresses of the k th layer, $S_{ij}^{(k)}$ are the components of the symmetric Piola–Kirchhoff stress tensor of the k th layer, $b_{ijlm}^{(k)}$ are the rigidities of the k th layer, p_i^- and p_i^+ are the external surface loads operating on the inner S^- and outer S^+ faces of the shell, $\mathbf{q}^{(k)} = q_v^{(k)} \mathbf{v} + q_t^{(k)} \mathbf{t} + q_3^{(k)} \mathbf{e}_3$ is the vector of external surface loads operating on the lateral surface of the k th layer Ω_k , and \mathbf{v} and \mathbf{t} are the normal and tangential unit vectors to the boundary contour $\Gamma \subset S$. Hereinafter, $k = \overline{1, N}$; $i, j, l, m = 1, 2, 3$; $\alpha, \beta, \gamma = 1, 2$.

Statement of the Problem

In constructing the theory of multilayer anisotropic shells with account of transverse compression, we use the Timoshenko kinematic hypothesis that the displacements are distributed linearly across the shell thickness [8, 9]:

$$u_i = N^-(\alpha_3)v_i^- + N^+(\alpha_3)v_i^+, \quad (1)$$

$$N^-(\alpha_3) = \frac{1}{h}(\delta^+ - \alpha_3), \quad N^+(\alpha_3) = \frac{1}{h}(\alpha_3 - \delta^-),$$

where $v_i^\pm(\alpha_1, \alpha_2)$ are the displacements of the faces S^\pm of the shell and $N^\pm(\alpha_3)$ are linear functions of the shell form.

Introducing displacements (1) into the deformation relations of the three-dimensional theory of elasticity [10] and assuming that the tangential components of the Green–Lagrange strain tensor vary linearly across the shell thickness, we come to the deformation relations of the geometrically nonlinear theory of Timoshenko-type shells [11]

$$\varepsilon_{ai}^{\text{GL}} = N^-(\alpha_3)(e_{ai}^- + \eta_{ai}^-) + N^+(\alpha_3)(e_{ai}^+ + \eta_{ai}^+), \quad \varepsilon_{33}^{\text{GL}} = e_{33} + \eta_{33}. \quad (2)$$

Here

$$\begin{aligned}
e_{\alpha\alpha}^{\pm} &= \frac{1}{\zeta_{\alpha}^{\pm}} \lambda_{\alpha}^{\pm}, \quad 2e_{12}^{\pm} = \frac{1}{\zeta_1^{\pm}} \omega_1^{\pm} + \frac{1}{\zeta_2^{\pm}} \omega_2^{\pm}, \quad 2e_{\alpha 3}^{\pm} = \frac{\zeta_{\alpha}^{\pm}}{\bar{\zeta}_{\alpha}} \beta_{\alpha} - \frac{1}{\bar{\zeta}_{\alpha}} \theta_{\alpha}^{\pm}, \quad e_{33} = \beta_3, \\
\eta_{\alpha\alpha}^{\pm} &= \frac{1}{2(\zeta_{\alpha}^{\pm})^2} [(\lambda_{\alpha}^{\pm})^2 + (\omega_{\alpha}^{\pm})^2 + (\theta_{\alpha}^{\pm})^2], \\
2\eta_{12}^{\pm} &= \frac{1}{\zeta_1^{\pm} \zeta_2^{\pm}} (\lambda_1^{\pm} \omega_2^{\pm} + \lambda_2^{\pm} \omega_1^{\pm} + \theta_1^{\pm} \theta_2^{\pm}), \\
2\eta_{\alpha 3}^{\pm} &= \frac{1}{\bar{\zeta}_{\alpha}} (\beta_{\alpha} \lambda_{\alpha}^{\pm} + \beta_{\gamma} \omega_{\alpha}^{\pm} - \beta_3 \theta_{\alpha}^{\pm}), \quad \eta_{33} = \frac{1}{2} (\beta_1^2 + \beta_2^2 + \beta_3^2), \\
\lambda_{\alpha}^{\pm} &= \frac{1}{A_{\alpha}} v_{\alpha, \alpha}^{\pm} + B_{\gamma} v_{\gamma}^{\pm} + k_{\alpha} v_3^{\pm}, \quad \omega_{\alpha}^{\pm} = \frac{1}{A_{\alpha}} v_{\gamma, \alpha}^{\pm} - B_{\gamma} v_{\alpha}^{\pm}, \\
\theta_{\alpha}^{\pm} &= -\frac{1}{A_{\alpha}} v_{3, \alpha}^{\pm} + k_{\alpha} v_{\alpha}^{\pm}, \quad \beta_i = \frac{1}{h} (v_i^+ - v_i^-), \quad B_{\alpha} = \frac{1}{A_1 A_2} A_{\gamma, \alpha} \quad (\gamma \neq \alpha), \\
\zeta_{\alpha}^{\pm} &= 1 + k_{\alpha} \delta^{\pm}, \quad \bar{\zeta}_{\alpha} = 1 + k_{\alpha} \bar{\delta}, \quad \bar{\delta} = \frac{1}{2} (\delta^- + \delta^+),
\end{aligned} \tag{3}$$

where $\bar{\delta}$ is the distance from the surface S to the midsurface \bar{S} , and the subscript after the comma means partial differentiation with respect to α_1 and α_2 coordinates. Deformation relations (2) and (3) are rather attractive from the viewpoint of their use in the finite-element method, since they *exactly* describe arbitrarily large displacements of the shell as a rigid body. The proof of this fundamental fact is given in [12].

Let us formulate contact conditions. We assume for definiteness that the contact of the shell with an absolutely rigid plane foundation occurs on a part of the external surface S_c^+ of the shell, in the absence of friction in the contact zone. If the contacting bodies do not penetrate into each other and the contact pressure q_c^+ is nonpositive, we have

$$g^+ - \left(\sum_i v_i^+ \mathbf{e}_i \right) \cdot \mathbf{n} \geq 0, \quad q_c^+ \leq 0, \tag{4}$$

where $g^+(\alpha_1, \alpha_2)$ is the initial clearance, i.e., the shortest distance from a point $M^+(\alpha_1, \alpha_2)$ of the shell belonging to the surface S_c^+ of the expected contact to the foundation, and $\mathbf{n} = \sum_i n_i \mathbf{e}_i$ is the unit normal vector to the foundation plane.

Inequalities (4) must be supplemented with the condition that the contact pressure is determined at the points which come into contact with the foundation, i.e., the equality

$$q_c^+ \left(g^+ - \sum_i n_i v_i^+ \right) = 0 \tag{5}$$

must be satisfied.

Hu–Washizu Functional

To solve the problem of contact interaction of a prestressed shell with an absolutely rigid foundation, we introduce a displacement-independent strain tensor, whose tangential and shear components vary across the shell thickness according to the linear law

$$\varepsilon_{ai}^{\text{AS}} = N^-(\alpha_3)E_{ai}^- + N^+(\alpha_3)E_{ai}^+, \quad \varepsilon_{33}^{\text{AS}} = E_{33} \quad (6)$$

and, taking into account approximations (1) and (2), present the Hu–Washizu mixed variational principle from [11, 13] in the form

$$\delta J_{\text{HW}} - \delta J_{\text{c}} = 0, \quad (7)$$

where

$$\begin{aligned} \delta J_{\text{c}} &= \iint_{S_{\text{c}}^+} \left[\left(\mathbf{g}^+ - \mathbf{m}^T \mathbf{v} - \frac{1}{\varepsilon} \lambda \right) \delta \lambda - \lambda \mathbf{m}^T \delta \mathbf{v} \right] \bar{\mu} d\alpha_1 d\alpha_2, \\ \delta J_{\text{HW}} &= \left[\iint_{\bar{S}} (\mathbf{H} - \mathbf{D}\mathbf{E})^T \delta \mathbf{E} + (\mathbf{E} - \mathbf{e} - \boldsymbol{\eta})^T \delta \mathbf{H} - \mathbf{H}^T \delta \mathbf{e} \right. \\ &\quad \left. - (\mathbf{H}^0 + \mathbf{H})^T \delta \boldsymbol{\eta} + \mathbf{P}^T \delta \mathbf{v} \right] \bar{\mu} d\alpha_1 d\alpha_2 + \int_{\bar{\Gamma}} \hat{\mathbf{H}}_{\Gamma}^T \delta \mathbf{v}_{\Gamma} (1 + k_N \bar{\delta}) ds, \\ \mathbf{v} &= [v_1^- \ v_1^+ \ v_2^- \ v_2^+ \ v_3^- \ v_3^+]^T, \quad \mathbf{v}_{\Gamma} = [v_v^- \ v_v^+ \ v_t^- \ v_t^+ \ v_3^- \ v_3^+]^T, \\ \mathbf{E} &= [E_{11}^- \ E_{11}^+ \ E_{22}^- \ E_{22}^+ \ 2E_{12}^- \ 2E_{12}^+ \ 2E_{13}^- \ 2E_{13}^+ \ 2E_{23}^- \ 2E_{23}^+ \ E_{33}]^T, \\ \mathbf{e} &= [e_{11}^- \ e_{11}^+ \ e_{22}^- \ e_{22}^+ \ 2e_{12}^- \ 2e_{12}^+ \ 2e_{13}^- \ 2e_{13}^+ \ 2e_{23}^- \ 2e_{23}^+ \ e_{33}]^T, \\ \boldsymbol{\eta} &= [\eta_{11}^- \ \eta_{11}^+ \ \eta_{22}^- \ \eta_{22}^+ \ 2\eta_{12}^- \ 2\eta_{12}^+ \ 2\eta_{13}^- \ 2\eta_{13}^+ \ 2\eta_{23}^- \ 2\eta_{23}^+ \ \eta_{33}]^T, \\ \mathbf{H}^0 &= [H_{11}^{0-} \ H_{11}^{0+} \ H_{22}^{0-} \ H_{22}^{0+} \ H_{12}^{0-} \ H_{12}^{0+} \ H_{13}^{0-} \ H_{13}^{0+} \ H_{23}^{0-} \ H_{23}^{0+} \ H_{33}^0]^T, \\ \mathbf{H} &= [H_{11}^- \ H_{11}^+ \ H_{22}^- \ H_{22}^+ \ H_{12}^- \ H_{12}^+ \ H_{13}^- \ H_{13}^+ \ H_{23}^- \ H_{23}^+ \ H_{33}]^T, \\ \hat{\mathbf{H}}_{\Gamma} &= [\hat{H}_{vv}^- \ \hat{H}_{vv}^+ \ \hat{H}_{vt}^- \ \hat{H}_{vt}^+ \ \hat{H}_{v3}^- \ \hat{H}_{v3}^+]^T, \quad \mathbf{P} = [-p_1^- \ p_1^+ \ -p_2^- \ p_2^+ \ -p_3^- \ p_3^+]^T, \\ \mathbf{m} &= [0n_1 \ 0n_2 \ 0n_3]^T, \quad \bar{\mu} = A_1 A_2 \bar{\zeta}_1 \bar{\zeta}_2. \end{aligned} \quad (8)$$

In relations (8), we have introduced the following designations: λ is the Lagrange multiplier (a contact pressure for the case of a plane foundation); ε is a regularizing parameter; k_N is the normal curvature of the contour $\Gamma \subset S$; \mathbf{v} is the column of displacements; \mathbf{v}_{Γ} is the column of displacements of faces of the shell in the coordinates v, t , and α_3 associated with the boundary contour $\bar{\Gamma} \subset \bar{S}$; \mathbf{E} is the column of independently introduced strains; \mathbf{e} and $\boldsymbol{\eta}$ are the columns characterizing the linear and nonlinear components of the Green–Lagrange strain tensor; \mathbf{P} is the column of surface loads; \mathbf{D} is the asymmetrical 11×11 matrix of elastic coefficients, whose elements are determined based on assumptions [8, 9] to overcome the Poisson locking; \mathbf{H} is

the column of resulting stresses; \mathbf{H}^0 is the column of resulting initial stresses; $\hat{\mathbf{H}}_{\Gamma}$ is the column of the resulting external surface loads operating on the lateral surface Ω of the shell, which are found from the formulas

$$\begin{aligned}
D_{ijlm}^{pq} &= \sum_k \int_{\delta_{k-1}}^{\delta_k} b_{ijlm}^{(k)} [N^-(\alpha_3)]^{2-p-q} [N^+(\alpha_3)]^{p+q} d\alpha_3 \quad (p, q = 0, 1), \\
H_{\alpha i}^{\pm} &= \sum_k \int_{\delta_{k-1}}^{\delta_k} S_{\alpha i}^{(k)} N^{\pm}(\alpha_3) d\alpha_3, \quad H_{33} = \sum_k \int_{\delta_{k-1}}^{\delta_k} S_{33}^{(k)} d\alpha_3, \\
H_{\alpha i}^{0\pm} &= \sum_k \int_{\delta_{k-1}}^{\delta_k} \tau_{\alpha i}^{(k)} N^{\pm}(\alpha_3) d\alpha_3, \quad H_{33}^0 = \sum_k \int_{\delta_{k-1}}^{\delta_k} \tau_{33}^{(k)} d\alpha_3, \\
\hat{H}_{\nu\kappa}^{\pm} &= \sum_k \int_{\delta_{k-1}}^{\delta_k} q_{\nu\kappa}^{(k)} N^{\pm}(\alpha_3) d\alpha_3 \quad (\kappa = \nu, t, 3).
\end{aligned} \tag{9}$$

In this case, it must be assumed in Eqs. (9) that $b_{\alpha\beta\gamma 3}^{(k)} = b_{\alpha 333}^{(k)} = 0$. We should note that mixed variational equation (7), (8) generalizes the corresponding equations given in [11, 13].

Algorithm of Numerical Solution of the Contact Problem

In variational equation (7), the vector-functions \mathbf{v} , \mathbf{E} , and \mathbf{H} and the Lagrange multiplier λ are independent functional variables; therefore, we must use independent approximations for them on each finite element. For displacements and the Lagrange multiplier, we employ the standard bilinear approximation

$$\mathbf{v} = \sum_r N_r(\xi_1, \xi_2) \mathbf{v}_r, \quad \lambda = \sum_r N_r(\xi_1, \xi_2) \lambda_r, \tag{10}$$

where $\mathbf{v}_r = [v_{1r}^-, v_{1r}^+, v_{2r}^-, v_{2r}^+, v_{3r}^-, v_{3r}^+]^T$ are the columns of nodal displacements, λ_r are the values of the Lagrange multiplier at the nodes of a finite element, $N_r(\xi_1, \xi_2)$ are linear shape functions, $\xi_\gamma = (\alpha_\gamma - d_\gamma^{\text{el}}) / l_\gamma^{\text{el}}$ are the normalized curvilinear coordinates of the element, d_γ^{el} are the center coordinates of the element, $2l_\gamma^{\text{el}}$ are the lengths of sides of the element, and $r = \overline{1, 4}$.

For deformations and resulting stresses, according to the method of double approximation [14, 15] generalized to the case of geometrical nonlinearity and transverse compression [11, 12], we have even simpler formulas:

$$\mathbf{E} = \sum_{r_1, r_2} \mathbf{Q}^{r_1 r_2} \mathbf{E}^{r_1 r_2} \xi_1^{r_1} \xi_2^{r_2}, \quad \mathbf{H} = \sum_{r_1, r_2} \mathbf{Q}^{r_1 r_2} \mathbf{H}^{r_1 r_2} \xi_1^{r_1} \xi_2^{r_2}, \quad \mathbf{H}^0 = \sum_{r_1, r_2} \mathbf{Q}^{r_1 r_2} \mathbf{H}^{0 r_1 r_2} \xi_1^{r_1} \xi_2^{r_2}. \tag{11}$$

Here,

$$\begin{aligned}
\mathbf{E}^{00} &= [E_{11}^{-00} \ E_{11}^{+00} \ E_{22}^{-00} \ E_{22}^{+00} \ 2E_{12}^{-00} \ 2E_{12}^{+00} \ 2E_{13}^{-00} \ 2E_{13}^{+00} \ 2E_{23}^{-00} \ 2E_{23}^{+00} \ E_{33}^{00}]^T, \\
\mathbf{E}^{01} &= [E_{11}^{-01} \ E_{11}^{+01} \ 2E_{13}^{-01} \ 2E_{13}^{+01} \ E_{33}^{01}]^T, \\
\mathbf{E}^{10} &= [E_{22}^{-10} \ E_{22}^{+10} \ 2E_{23}^{-10} \ 2E_{23}^{+10} \ E_{33}^{10}]^T, \\
\mathbf{E}^{11} &= [E_{33}^{11}], \quad \mathbf{H}^{11} = [H_{33}^{11}],
\end{aligned} \tag{12}$$

$$\mathbf{H}^{00} = [H_{11}^{-00} \ H_{11}^{+00} \ H_{22}^{-00} \ H_{22}^{+00} \ H_{12}^{-00} \ H_{12}^{+00} \ H_{13}^{-00} \ H_{13}^{+00} \ H_{23}^{-00} \ H_{23}^{+00} \ H_{33}^{00}]^T,$$

$$\mathbf{H}^{01} = [H_{11}^{-01} \ H_{11}^{+01} \ H_{13}^{-01} \ H_{13}^{+01} \ H_{33}^{01}]^T, \quad \mathbf{H}^{10} = [H_{22}^{-10} \ H_{22}^{+10} \ H_{23}^{-10} \ H_{23}^{+10} \ H_{33}^{10}]^T,$$

$$\mathbf{Q}^{01} = \begin{bmatrix} 1 & 0 & 0 & 0 & 0 \\ 0 & 1 & 0 & 0 & 0 \\ 0 & 0 & 0 & 0 & 0 \\ 0 & 0 & 0 & 0 & 0 \\ 0 & 0 & 0 & 0 & 0 \\ 0 & 0 & 0 & 0 & 0 \\ 0 & 0 & 1 & 0 & 0 \\ 0 & 0 & 0 & 1 & 0 \\ 0 & 0 & 0 & 0 & 0 \\ 0 & 0 & 0 & 0 & 0 \\ 0 & 0 & 0 & 0 & 1 \end{bmatrix}, \quad \mathbf{Q}^{10} = \begin{bmatrix} 0 & 0 & 0 & 0 & 0 \\ 0 & 0 & 0 & 0 & 0 \\ 1 & 0 & 0 & 0 & 0 \\ 0 & 1 & 0 & 0 & 0 \\ 0 & 0 & 0 & 0 & 0 \\ 0 & 0 & 0 & 0 & 0 \\ 0 & 0 & 0 & 0 & 0 \\ 0 & 0 & 0 & 0 & 0 \\ 0 & 0 & 1 & 0 & 0 \\ 0 & 0 & 0 & 1 & 0 \\ 0 & 0 & 0 & 0 & 1 \end{bmatrix}, \quad \mathbf{Q}^{11} = \begin{bmatrix} 0 \\ 0 \\ 0 \\ 0 \\ 0 \\ 0 \\ 0 \\ 0 \\ 0 \\ 0 \\ 1 \end{bmatrix}, \quad (12)$$

where \mathbf{Q}^{00} is the 11×11 unit matrix, and the columns $\mathbf{H}^{0r_1r_2}$ are determined similarly to $\mathbf{H}^{r_1r_2}$. Hereinafter, the superscripts r_1 and r_2 take the values 0 or 1.

Introducing approximations (10)-(12) into variational equation (7), (8) and using the standard procedure of the mixed model of finite-element method, we come to the following equations of equilibrium for the finite element:

$$\mathbf{E}^{r_1r_2} = (\mathbf{Q}^{r_1r_2})^T (\mathbf{B}^{r_1r_2} + \mathbf{R}^{r_1r_2} \mathbf{V}) \mathbf{V}, \quad \mathbf{H}^{r_1r_2} = (\mathbf{Q}^{r_1r_2})^T \mathbf{DQ}^{r_1r_2} \mathbf{E}^{r_1r_2}, \quad (13)$$

$$\sum_{r_1, r_2} \frac{1}{3^{r_1+r_2}} [(\mathbf{B}^{r_1r_2} + 2\mathbf{R}^{r_1r_2} \mathbf{V})^T \mathbf{Q}^{r_1r_2} \mathbf{H}^{r_1r_2} + 2(\mathbf{R}^{r_1r_2} \mathbf{V})^T \mathbf{Q}^{r_1r_2} \mathbf{H}^{0r_1r_2} + \mathbf{L}^{r_1r_2} \mathbf{\Lambda}] = \mathbf{F},$$

where $\mathbf{V} = [v_1^T \ v_2^T \ v_3^T \ v_4^T]^T$ is the column of nodal displacements of the element; $\mathbf{\Lambda} = [\lambda_1 \ \lambda_2 \ \lambda_3 \ \lambda_4]^T$ is the column of nodal values of the Lagrange multiplier; \mathbf{F} is the column of central loads; $\mathbf{L}^{r_1r_2}$ are 24×4 matrices corresponding to the contact interaction of the element; $\mathbf{B}^{r_1r_2}$ are 11×24 matrices describing the linear components of the Green–Lagrange strain tensor; $\mathbf{R}^{r_1r_2}$ are three-dimensional $11 \times 24 \times 24$ arrays describing the nonlinear components of the Green–Lagrange strain tensor, where $\mathbf{R}^{r_1r_2} \mathbf{V}$ are 11×24 matrices, whose elements are calculated from the formulas

$$(\mathbf{R}^{r_1r_2} \mathbf{V})_{np} = \sum_q R_{npq}^{r_1r_2} V_q, \quad R_{npq}^{r_1r_2} = R_{nqp}^{r_1r_2} \quad (n = \overline{1, 11}; \quad p, q = \overline{1, 24}).$$

Let us supplement Eqs. (13) with relations which, according to Eqs. (4) and (5), are responsible for satisfying the contact conditions. In the contact zone ($\rho \in I_c$, where $I_c \subset \{1, 2, 3, 4\}$), the conditions

$$g_\rho^+ - \mathbf{m}_\rho^T \mathbf{v}_\rho - \frac{1}{\varepsilon} \lambda_\rho = 0, \quad (14.1)$$

$$\lambda_\rho \leq 0, \quad (14.2)$$

must hold, and outside the contact zone ($\rho \notin I_c$), the conditions

$$g_\rho^+ - \mathbf{m}_\rho^T \mathbf{v}_\rho \geq 0, \quad (15.1)$$

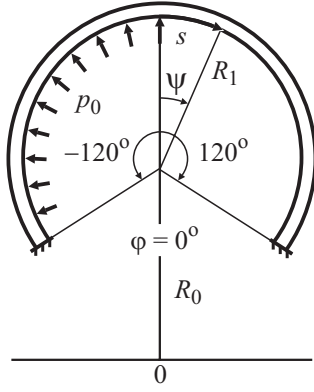


Fig. 2

Fig. 2. Angle-ply toroidal shell (bias tire).

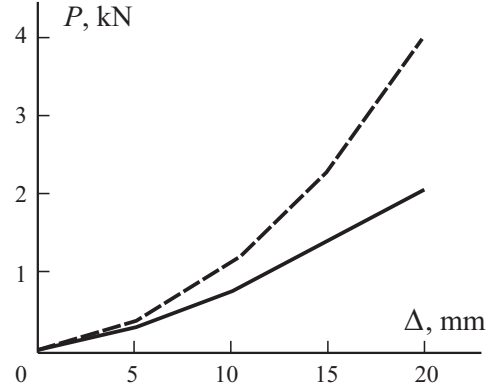


Fig. 3

Fig. 3. Load–deflection curve P – Δ for the bias tire in linear (---) and nonlinear (—) formulations.

$$\lambda_p = 0, \quad (15.2)$$

must be satisfied, where g_r^+ are the clearances at the nodes of the finite element and $\mathbf{m}_r = [0n_{1r} \ 0n_{2r} \ 0n_{3r}]^T$ are the columns describing the unit normal vectors to the foundation plane at the nodes.

Excluding the columns $\mathbf{E}^{r_1 r_2}$ and $\mathbf{H}^{r_1 r_2}$ from Eqs. (13), we come to the system of nonlinear equations

$$\sum_{r_1, r_2} \frac{1}{3^{r_1 + r_2}} [(\mathbf{B}^{r_1 r_2} + 2\mathbf{R}^{r_1 r_2} \mathbf{V})^T \mathbf{Q}^{r_1 r_2} (\mathbf{Q}^{r_1 r_2})^T \mathbf{D} \mathbf{Q}^{r_1 r_2} (\mathbf{Q}^{r_1 r_2})^T \times (\mathbf{B}^{r_1 r_2} + \mathbf{R}^{r_1 r_2} \mathbf{V}) \mathbf{V} + 2(\mathbf{R}^{r_1 r_2} \mathbf{V})^T \mathbf{Q}^{r_1 r_2} \mathbf{H}^{0r_1 r_2} + \mathbf{L}^{r_1 r_2} \mathbf{\Lambda}] = \mathbf{F}, \quad (16)$$

which can be solved together with conditions (14) and (15).

Next, we use the standard procedure of assembling the finite elements to obtain a system of nonlinear equations in the global vector of nodal displacements, which will not be considered here.

For solving the problem, we used the trial-and-error method, which consists in the following. First, an initial approximation of the contact zone is assigned, and the nonlinear system of equations (14.1), (15.2), and (16) is solved by the Newton–Raphson method, and then, for each node, the fulfillment of inequalities (14.2) and (15.1) is checked. If inequality (14.2) does not hold, the node is removed from the contact zone. If inequality (15.1) is not fulfilled, the node is added to the contact zone.

Numerical Results and Their Discussion

As an example, we will consider the problem on compression of a four-layer angle-ply rubber-cord toroidal shell of circular cross section on a rigid foundation (Fig. 2). With the help of this shell, we will model a bias tire. The initial characteristics of elementary rubber-cord layers are as follows [16]: $E_L = 510.45$ MPa, $E_T = 6.91$ MPa, $G_{LT} = 2.33$ MPa, $G_{TT} = 1.77$ MPa, $\nu_{LT} = 0.46$, and $\nu_{TT} = 0.95$, where the subscripts L and T correspond to the reinforcement and transverse directions, re-

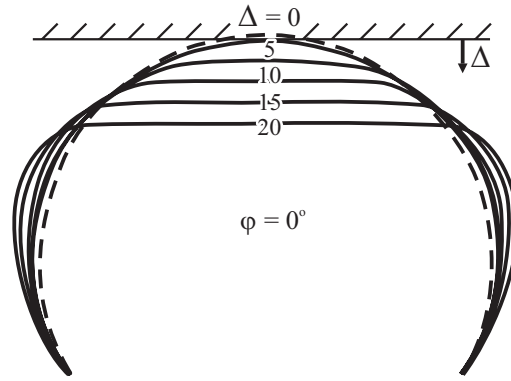


Fig. 4. Deformed profiles of the bias tire at $\varphi = 0^\circ$ and different values of Δ (numbers at the curves).

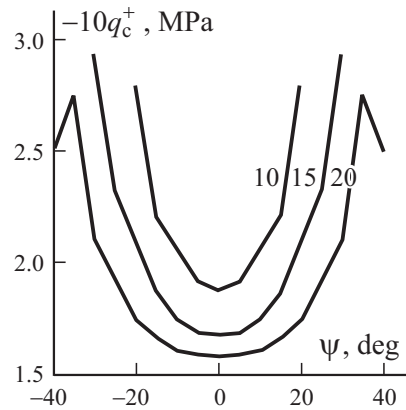


Fig. 5. Distribution of contact pressure at $\varphi = 0^\circ$ and different values of Δ (numbers at the curves).

spectively. Let the thickness of the elementary rubber-cord layer be $h_k = 1.2$ mm, the total thickness of the shell $h = 4.8$ mm, and the orientation of the rubber-cord layers $\gamma_k = (-1)^{k-1} \gamma$, where $\gamma = 52^\circ$ and $k = \overline{1, 4}$. As the reference surface, we take the internal surface of the tire, which is formed by rotating a circumference of radius $R_1 = 50$ mm. The distance from the rotation axis to the equator of the reference surface of the tire is $R_0 = 250$ mm. In our numerical calculations, it was assumed that the cross sections of the tire with the coordinates $\psi = \pm 120^\circ$ were rigidly fixed.

First, based on the numerical algorithm described in [12], the tire was calculated for the action of an internal pressure $p_0 = 0.15$ MPa. Then, we solved the contact problem using this algorithm. We should note that, in view of anisotropy, the symmetry conditions were not taken into account, and irregular meshes of 42×40 elements in the meridional and circumferential directions were used. For the regularization parameter, we chose $\varepsilon = 10^4$, which is optimum for the given class of problems. The results of numerical calculations for the loading characteristic of the tire, based on the geometrically linear (dashed curve) and nonlinear (continuous curve) theories of shells, are given in Fig. 3, where P is the compressive force on the supporting plane and Δ is the displacement of the plane. As seen from the figure, the linear theory of shells gives a twofold overestimated value for the loading characteristic of the tire. Figure 4 shows the deformed profiles of the tire outer contour for the central meridional

TABLE 1. Distribution of Contact Pressure $-10q_c^+$ (MPa) over the Contact Zone at $\Delta = 20$ mm for Different Values of 3ϕ (deg)

| ψ , deg | -45 | -40 | -35 | -30 | -25 | -20 | -15 | -10 | -5 | 0 | 5 | 10 | 15 | 20 | 25 | 30 | 35 | 40 | 45 |
|--------------|------|------|------|------|------|------|------|------|------|------|------|------|------|------|------|------|------|------|------|
| -40 | | | | | | | 1.37 | 2.07 | 2.24 | 2.49 | 2.31 | 2.18 | 1.52 | 0.30 | | | | | |
| -35 | | | | 1.32 | 2.58 | 3.34 | 2.64 | 2.86 | 2.37 | 2.75 | 2.42 | 2.88 | 2.78 | 3.27 | 2.93 | 1.69 | | | |
| -30 | | | 2.84 | 2.70 | 2.55 | 2.17 | 2.31 | 2.11 | 2.24 | 2.10 | 2.26 | 2.16 | 2.32 | 2.29 | 2.54 | 2.78 | 3.13 | | |
| -25 | | 2.88 | 2.39 | 2.30 | 2.14 | 2.09 | 1.96 | 1.96 | 1.89 | 1.93 | 1.90 | 1.97 | 1.98 | 2.09 | 2.17 | 2.33 | 2.45 | 3.14 | |
| -20 | 2.53 | 2.16 | 2.26 | 2.02 | 1.92 | 1.83 | 1.80 | 1.76 | 1.76 | 1.74 | 1.76 | 1.76 | 1.80 | 1.84 | 1.93 | 2.03 | 2.28 | 2.19 | 2.92 |
| -15 | 2.39 | 2.04 | 2.01 | 1.86 | 1.78 | 1.73 | 1.69 | 1.67 | 1.66 | 1.66 | 1.66 | 1.67 | 1.69 | 1.73 | 1.79 | 1.86 | 2.02 | 2.04 | 2.46 |
| -10 | 2.31 | 1.87 | 1.90 | 1.77 | 1.70 | 1.66 | 1.63 | 1.61 | 1.61 | 1.60 | 1.60 | 1.61 | 1.63 | 1.66 | 1.70 | 1.78 | 1.90 | 1.86 | 2.38 |
| -5 | 2.21 | 1.82 | 1.83 | 1.72 | 1.66 | 1.63 | 1.60 | 1.59 | 1.58 | 1.57 | 1.58 | 1.58 | 1.60 | 1.62 | 1.66 | 1.72 | 1.83 | 1.81 | 2.24 |
| 0 | 2.20 | 1.79 | 1.82 | 1.70 | 1.65 | 1.62 | 1.59 | 1.58 | 1.57 | 1.56 | 1.57 | 1.58 | 1.59 | 1.62 | 1.65 | 1.70 | 1.82 | 1.79 | 2.20 |
| 5 | 2.24 | 1.81 | 1.83 | 1.72 | 1.66 | 1.62 | 1.60 | 1.58 | 1.58 | 1.57 | 1.58 | 1.59 | 1.60 | 1.63 | 1.66 | 1.72 | 1.83 | 1.82 | 2.21 |
| 10 | 2.38 | 1.86 | 1.90 | 1.78 | 1.70 | 1.66 | 1.63 | 1.61 | 1.60 | 1.60 | 1.61 | 1.61 | 1.63 | 1.66 | 1.70 | 1.77 | 1.90 | 1.87 | 2.31 |
| 15 | 2.46 | 2.04 | 2.02 | 1.86 | 1.79 | 1.73 | 1.69 | 1.67 | 1.66 | 1.66 | 1.66 | 1.67 | 1.69 | 1.73 | 1.78 | 1.86 | 2.01 | 2.04 | 2.39 |
| 20 | 2.92 | 2.19 | 2.28 | 2.03 | 1.93 | 1.84 | 1.80 | 1.76 | 1.76 | 1.74 | 1.76 | 1.76 | 1.80 | 1.83 | 1.92 | 2.02 | 2.26 | 2.16 | 2.53 |
| 25 | | 3.14 | 2.45 | 2.33 | 2.17 | 2.09 | 1.98 | 1.97 | 1.90 | 1.93 | 1.89 | 1.96 | 1.96 | 2.09 | 2.14 | 2.30 | 2.39 | 2.88 | |
| 30 | | | 3.13 | 2.78 | 2.54 | 2.29 | 2.32 | 2.16 | 2.26 | 2.10 | 2.24 | 2.11 | 2.31 | 2.17 | 2.55 | 2.70 | 2.84 | | |
| 35 | | | | 1.69 | 2.93 | 3.27 | 2.78 | 2.88 | 2.42 | 2.75 | 2.37 | 2.86 | 2.64 | 3.34 | 2.58 | 1.32 | | | |
| 40 | | | | | | 0.30 | 1.52 | 2.18 | 2.31 | 2.49 | 2.24 | 2.07 | 1.37 | | | | | | |

section $\varphi=0^\circ$, where φ is the circumferential coordinate. In this case, the dashed profile corresponds to the unloaded tire. Figure 5 illustrates the contact pressure q_c^+ as a function of the meridional coordinate ψ for three values of Δ .

More complete data on the contact pressure and the magnitude of the contact spot at $\Delta=20$ mm are given in Table 1, whence it follows that the symmetry conditions for the contact pressure in the bias tire are broken. As is seen, we have a *central symmetry* here. Although the effect of anisotropy on the distribution of contact pressure and the sizes of the contact spot is not so significant for engineering calculations, for the mechanics of composite structures, it is still of principal importance.

As our calculations have shown, the influence of anisotropy on the stressed state of the tire is considerable. However, because of the limited volume of the paper, this analysis is not presented here.

Acknowledgments. The study was financially supported by the Russian Fund for Basic Research (Project code 04-01-00070).

REFERENCES

1. E. I. Grigolyuk and G. M. Kulikov, Investigation Methods for the Stress-Strain State of Multilayer Composite Shells with Application to the Mechanics of Pneumatic Tires, Scientific and Technical Progress in Mechanical Engineering, Iss. 39 [in Russian], MTsNTI, Inst. Mashinoved. RAN (1993).
2. R. A. Ridha and M. Theves, "Advances in tire mechanics," in: IRC 94. Vol. 1, Moscow (1994), pp. 54-126.
3. A. K. Noor and K. T. Danielson, "Finite elements developed in cylindrical coordinates for three-dimensional tire analysis," Tire Sci. Technol., **25**, No. 1, 2-28 (1997).
4. K. O. Kim, J. A. Tanner, A. K. Noor, and M. P. Robinson, Computational Methods for Frictionless Contact with Application to Space Shuttle Orbiter Nose-Gear Tires, NASA TP-3073 (1991).
5. J. A. Tanner, V. J. Martinson, and M. P. Robinson, "Static frictional contact of the space shuttle nose-gear tire," Tire Sci. Technol., **22**, No. 4, 242-272 (1994).
6. E. I. Grigolyuk, G. M. Kulikov, and S. V. Plotnikova, "A contact problem for a multilayer anisotropic shell of revolution," in: Problems of Tires and Rubber-Cord Composites. Vol. 1 [in Russian], NIIShP, Moscow (2000), pp. 189-197.
7. L. O. Faria, J. T. Oden, B. Yavari, W. W. Tworzydlo, J. M. Bass, and E. B. Becker, "Tire modeling by finite elements," Tire Sci. Technol., **20**, No. 1, 33-56 (1992).
8. G. M. Kulikov, "Analysis of initially stressed multilayered shells," Int. J. Solids Struct., **38**, Nos. 26-27, 4535-4555 (2001).
9. G. M. Kulikov and S. V. Plotnikova, "Investigation of locally loaded multilayer shells by a mixed finite-element method. 1. Geometrically linear statement," Mech. Compos. Mater., **38**, No. 5, 397-406 (2002).
10. V. V. Novozhilov, Theory of Elasticity [in Russian], Sudpromgiz, Leningrad (1958).
11. G. M. Kulikov and S. V. Plotnikova, "Investigation of locally loaded multilayer shells by a mixed finite-element method. 2. Geometrically nonlinear statement," Mech. Compos. Mater., **38**, No. 6, 539-546 (2002).
12. G. M. Kulikov and S. V. Plotnikova, "Non-linear strain-displacement equations exactly representing large rigid-body motions. Pt. I. Timoshenko-Mindlin shell theory," Comput. Meth. Appl. Mech. Eng., **192**, Nos. 7-8, 851-875 (2003).
13. G. M. Kulikov and S. V. Plotnikova, "A contact problem for a geometrically nonlinear shell of Timoshenko type," Prikl. Matem. Mekh., **67**, No. 6, 940-953 (2003).
14. G. Wempner, D. Talaslidis, and C. M. Hwang, "A simple and efficient approximation of shells via finite quadrilateral elements," Trans. ASME. J. Appl. Mech., **49**, No. 1, 115-120 (1982).
15. A. I. Golovanov and M. S. Kornishin, Introduction to the Method of Finite Elements in Statics of Thin Shells [in Russian], KFTI Akad. Nauk SSSR, Kazan' (1989).
16. E. I. Grigolyuk and G. M. Kulikov, Multilayer Reinforced Shells. Calculation of Pneumatic Tires [in Russian], Mashinostroenie, Moscow (1988).